Genes &
Diseases
an international journal for molecular and translational medicine

FULL LENGTH ARTICLE

Hippocampal overexpression of TREM2 ameliorates high fat diet induced cognitive impairment and modulates phenotypic polarization of the microglia

Min Wu [a,b,1], Maolin Liao [a,b,1], Rongfeng Huang [a,b], Chunxiu Chen [b,c], Tian Tian [d], Hongying Wang [a,b], Jiayu Li [a,b], Jibin Li [c], Yuxiang Sun [e], Chaodong Wu [e], Qifu Li [a], Xiaoqiu Xiao [a,b,*]

[a] *Department of Endocrinology, The First Affiliated Hospital of Chongqing Medical University, Chongqing 400016, PR China*
[b] *The Chongqing Key Laboratory of Translational Medicine in Major Metabolic Diseases, The First Affiliated Hospital of Chongqing Medical University, Chongqing 400016, PR China*
[c] *Department of Nutrition and Food Hygiene, School of Public Health and Management, Chongqing Medical University, Chongqing 400016, PR China*
[d] *Department of Neurology, Affiliated Hospital of Guizhou Medical University, Guiyang, Guizhou 550004, PR China*
[e] *Department of Nutrition and Food Science, Texas A&M University, College Station, TX 77843, USA*

Abstract Type 2 diabetes mellitus (T2DM) and Alzheimer's disease (AD) share several common pathophysiological features. Rare variants of triggering receptor expressed on myeloid cells 2 (TREM2) increase the risk of developing AD, suggesting the involvement of TREM2 and innate immunity in AD development. It is still unknown whether TREM2 is related to cognitive impairment in T2DM. Here, we investigated the effects of the hippocampal overexpression of TREM2 on cognitive in long-term high-fat diet (HFD)-fed mice. Male C57BL/6J mice were maintained on HFD for 50 weeks. TREM2 was overexpressed in the hippocampus 36 weeks after HFD feeding using adeno-associated virus vector (AAV)-mediated gene delivery. The results showed that the HFD feeding induced rapid and persistent weight gain, glucose intolerance and

* Corresponding author. Department of Endocrinology, The First Affiliated Hospital of Chongqing Medical University, Chongqing 400016, PR China.
  E-mail address: bshaw2001@163.com (X. Xiao).
  Peer review under responsibility of Chongqing Medical University.
[1] Equal contributors.

significant impairments in learning and memory. Compared with AAV-con, AAV-TREM2 significantly ameliorated cognitive impairment without altering body weight and glucose homeostasis in HFD mice. The overexpression of TREM2 upregulated the synaptic proteins spinophilin, PSD95 and synaptophysin, suggesting the improvement in synaptic transmission. Dendritic complexity and spine density in the CA1 region were rescued after TREM2 overexpression. Furthermore, TREM2 markedly increased the number of iba-1/Arg-1-positive microglia in the hippocampus, suppressed neuroinflammation and microglial activation. In sum, hippocampal TREM2 plays an important role in improving HFD-induced cognitive dysfunction and promoting microglial polarization towards the M2 anti-inflammatory phenotype. Our study also suggests that TREM2 might be a novel target for the intervention of obesity/diabetes-associated cognitive decline.

Introduction

Rare variants of triggering receptor expressed on myeloid cells 2 (TREM2) have been identified as risk factors for Alzheimer's disease (AD), and carriers of these rare variants exhibit a 2- to 3-fold increased the risk of developing AD.[1,2] In the brain, TREM2 is specifically enriched on microglial cells (over 300-fold compared to expression on astrocytes) and is also one of the most highly expressed receptors in microglia.[3] Microglial cells account for 5−10% of the total cell population in the brain and play an important role in the innate immune system in the central nervous system (CNS).[4] Both *in vitro* and *in vivo* studies have illustrated that TREM2 might protect against neurodegeneration by promoting phagocytosis and controlling detrimental inflammation.[5,6] Furthermore, the activation of TREM2 is revealed to reprogram microglia from a homeostatic phenotype to a neuroprotective phenotype.[7]

Type 2 diabetes mellitus (T2DM) and AD share several common age-related pathophysiological features.[8] Neuroinflammation is closely related to the pathogenesis of AD and obesity/T2DM. The hippocampus, the main functional area involved in learning and memory, is particularly sensitive to HFD.[9,10] As the sentinel immune cells of the CNS, microglial cells are generally activated after chronic HFD consumption and then mediate inflammation in the hippocampus. Synaptic loss in obesity is thought to be mediated by microglia, and microglial overactivation is thought to be a major cause of inflammation-mediated brain damage.[11] Therefore, therapeutic interventions targeting neuroinflammation are considered to be a promising approach for preventing the progression of obesity/diabetes cognitive impairment.

The activation of microglia can originate a plethora of functional phenotypes, encompassing the classic M1 proinflammatory and the alternative M2 anti-inflammatory phenotypes.[12,13] Therapeutic strategies of inhibiting microglia M1 polarization or promoting M2 polarization may be an exciting approach for inflammatory related diseases of central nervous system. Recently, several studies have suggested the neuroprotective effect of TREM2 in rodent models of AD, Parkinson's disease (PD) and ischemic stroke, which are related to the anti-neuroinflammation effect and the regulation of microglial polarization.[14−16] However, it remains unclear whether the activation of TREM2 signalling attenuates obesity/diabetes-related cognitive impairment. Here, we aim to explore the role of the hippocampal overexpression of TREM2 in the regulation of cognitive functions in long-term HFD-fed mice and the related mechanism. We applied a long-term HFD feeding protocol to induce obesity/diabetes and cognitive impairment in mice and then overexpressed TREM2 in the bilateral hippocampus. The results show that TREM2 overexpression normalizes dendritic complexity, synaptic ultrastructure, and the expression of synaptic proteins and finally rescues cognitive impairment in HFD-fed mice. Moreover, TREM2 promotes microglial M2 polarization and inhibits classical activation of microglia, the activation of NF-κB pathway and neuroinflammation, which may contribute to its protective effects in HFD-fed mice.

Materials and methods

Animals and diet

Male C57BL/6J mice (8 weeks of age) were housed five per cage and fed a HFD (60% energy from fat, 20% energy from protein and 20% energy from carbohydrates, D12492, Research Diets, Inc.) or normal control diet (NCD, 10% energy from fat, 20% energy from protein and 70% energy from carbohydrates, D12450B, Research Diets, Inc.), and water was available *ad libitum*. Body weight was measured every 1−2 weeks, and other treatments were performed at designated times according to the experimental timeline (Fig. 1). The Animal Care and Management Committee of Chongqing Medical University approved the entire study protocol. All animal experiments were conducted in accordance with the Guide for the Care and Use of Laboratory Animals of the National Institutes of Health.

Preparation of adeno-associated virus particles and stereotaxic surgery

An adeno-associated virus (AAV) engineered to overexpress mouse TREM2 (NCBI ID: NM_031254.3) under the microglial specific CD68 promoter and a control AAV were provided by
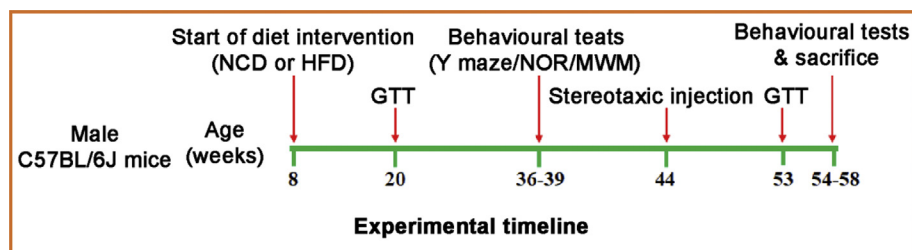
Figure 1 Experimental timeline. Male mice were placed on a high fat diet (HFD) or normal control diet (NCD) diet at 8 weeks of age. Mice were subjected a glucose tolerance tests (GTT) at 20 weeks and 53 weeks of age. Bilateral hippocampal stereotaxic injection was handled at 44 weeks of age. Behavioural performance was assessed at 36 weeks and 54 weeks of age by using the Y maze, novel object recognition test (NOR), and Morris water maze (MWM). Finally, mice were perfused, and brains collected for further experiments.

GeneChem Biotech. Co. Ltd. (Shanghai, China). The titer for AAV particles containing TREM2 vector (AAV-TREM2) was 1.63×10^{12} V G./ml. the titer for control virus (AAV-con) was 1.01×10^{12} V G./ml. Stereotactic intracerebral injection was performed by means of an automated stereotaxic injection system (RWD, Shenzhen, China) equipped with a 5 μl microsyringe (RWD, Shenzhen, China). Mice were anaesthetized with continuous isoflurane throughout the duration of surgery. Viral particles were bilaterally delivered into the hippocampus (1 μl per side) at a rate of 0.2 μl/min. Following virus delivery, the syringe was left in place for 5 min before being slowly withdrawn to limit reflux. Coordinates for injection (in mm) relative to Bregma were −2.0 anteroposterior (AP); ±1.5 mediolateral (ML); and −1.6 dorsoventral (DV).[17]

Behavioural tests

Behavioural tests were performed after 28 weeks of HFD feeding (before AAV-TREM2 delivery) and after 46 weeks of HFD feeding (after AAV-TREM2 delivery). All mice from each group were tested with the Y maze, novel object recognition (NOR) test and Morris water maze (MWM). The mice were transferred into the testing room 30 min before the Y maze and NOR tests and 2 days before the MWM test for acclimation. For the NOR test and Y maze, the apparatuses were wiped down with 50% ethanol between tests to minimize olfactory cues. For the Y maze, we measured spontaneous alternations to evaluate short-term spatial memory performance. The mice were gently transferred to the starting arm (length × width × height (in cm): 30 × 7 × 15) and then subjected to a single 8-min trial in which they were allowed to move freely through all three arms of the Y maze. The paths of the mice were recorded by a digital video recorder for further analysis by using Ethovision XT (Noldus Information Technology, Wageningen, The Netherlands). A successful alternation was defined as entry into all three arms consecutively. The number of maximum alternations was therefore the total number of arm entries minus 2, and the alternation rate was calculated as actual alternations/maximum alternations × 100%, as described previously.[18]

The NOR test involved three sessions: habituation, familiarization and the recognition memory test.[19] A long habituation procedure (repeated for 3 consecutive days) was adopted, and the mice were allowed to freely explore an empty open-field box (length × width × height (in cm): 44 × 44 × 30) for 5 min. A familiarization session, in which each mouse was placed in the same open-field box containing two identical objects for 5 min, was performed the next day. Recognition memory was tested after 24 h. One familiar object was replaced by a novel object with an obviously different shape, colour and texture, and the exploration time was set as 7 min. Based on the video, the time spent exploring and sniffing each object was analysed by Ethovision XT. Exploration was defined as the mouse pointing its nose towards the object at a distance less than or equal to 2 cm. The preference index was used to evaluate recognition memory, and it was calculated as the ratio between the time spent exploring the novel object and the total time spent exploring both objects (TN/(TN + TF), with TN being equal to the time spent exploring the novel object and TF being equal to the time spent exploring the familiar object).

Spatial learning and memory were evaluated by the Morris water maze (MWM).[20] A 120-cm circular pool was filled with water, which was opacified with milk powder and kept at 23 ± 1 °C. A platform (7 cm in diameter) was hidden 1 cm beneath the surface of the water in the northwest (NW) quadrant (southwest in the second test). The memory acquisition phase consisted of 4 × 60 s trials per day with four different starting locations in the different quadrants around the edge of the tank. A trial was completed when the mouse reached the platform, and the mice were allowed to stay on the platform for 15 s. If the mouse failed to climb on the platform within 60 s, it was manually guided to the platform and held on the platform for 15 s. Acquisition training was performed for five consecutive days, and the latency for each mouse to find the hidden platform was recorded. The probe test was conducted on the sixth day; the platform was removed, and the mice were allowed to explore for 60 s. Swimming speed, escape latency, the path length in the target quadrant and the number of platform crosses were analysed with Ethovision XT.

RNA extraction and RT-qPCR

Total RNA was extracted from the hippocampus using Trizol reagent (Invitrogen). RNA quantity and quality were

determined by using a NanoDrop 2000 Spectrophotometer (Thermo Scientific). Complementary DNA was synthesized from 1 μg of total RNA with EvoScript Universal cDNA Master (Roche). The resulting cDNA was diluted and used for real-time reverse transcription PCR using a BIO-RAD PCR system. The primer sequences for the genes are listed in Table S1. The 10-μl reaction contained the following: 5 μl of SYBR Green Fast Master Mix (Roche); 1 μl of forward primer and 1 μl of reverse primer; and 3 μl of diluted cDNA. The reaction steps followed the manufacturer's recommendations.

Western blotting

Total protein from the mouse hippocampus was extracted using RIPA Lysis and Extraction Buffer (Thermo Scientific) premixed with protease inhibitor cocktail and PhosSTOP (Roche). The samples were centrifuged for 15 min at 12,000 rpm at 4 °C, and the supernatant was extracted. The protein concentration was determined by a BCA assay (Beyotime, Shanghai, China) with Multiskan GO (Thermo Scientific).

Protein samples were separated by SDS-PAGE and then transferred to 0.45 mm polyvinylidene difluoride (PVDF) membranes (Millipore). The following primary antibodies were used: anti-β-actin mouse monoclonal antibody (1:1000, Cell Signaling Technology, CST), anti-α-tubulin mouse monoclonal antibody (1:10,000, Proteintech), anti-TREM2 goat polyclonal antibody (1:1000, Abcam), anti—NF—κB p65 rabbit monoclonal antibody (1:1000, CST), anti-phospho—NF—κB p65 rabbit monoclonal antibody (1:1000, CST), anti-IkBα mouse monoclonal antibody (1:1000, CST), anti-phospho-IkBα (Ser32) rabbit monoclonal antibody (1:1000, CST), anti-synaptophysin mouse monoclonal antibody (1:4000, Santa Cruz), anti-PSD95 mouse monoclonal antibody (1:5000, Santa Cruz), and anti-spinophilin rabbit polyclonal antibody (1:2000, Proteintech). The following secondary antibodies were used: rabbit anti-goat IgG (1:5000, Proteintech), goat anti-mouse IgG (1:5000, Bosterbio), and goat anti-rabbit IgG (1:5000, Bosterbio). The membranes were visualized using an ECL reagent (Thermo Scientific) and a Fusion FX Spectra system (Vilber Lourmat).

Immunofluorescence and image analysis

Mice were anaesthetized with isoflurane and transcardially perfused with 0.1 M PBS followed by ice cold 4% paraformaldehyde (PFA). For sectioning, the brains were embedded in Tissue-Tek O.C.T. Compound (Sakura) and cut into 20-μm sections. The brain sections were stored at −80 °C.

For double-labelling immunofluorescence, antigen retrieval was performed using boiling citrate buffer (pH 6.0) for 15 min. The sections were then blocked in PBS with 0.3% Triton X-100 and 10% normal donkey serum for 1 h at room temperature and incubated in primary antibody at 4 °C overnight. The next day, the sections were washed with PBS (5 min × 3 times) and incubated with secondary antibodies for 1 h at RT in the dark. The nuclei were stained with DAPI (Beyotime, Shanghai, China), and the sections were

mounted with Antifade Mounting Medium (Solarbio, Beijing, China). The following primary antibodies were used: goat anti-iba1 (1:400, Abcam), sheep anti-TREM2 (1:100, R&D), rabbit anti-Arg-1 (1:100, CST), and rabbit anti-iNOS (1:100, Proteintech). The secondary antibodies were Alexa 647-conjugated donkey anti-goat (1:400, Abcam), Alexa 555-conjugated donkey anti-rabbit (1:400, Abcam), and Alexa 555-conjugated donkey anti-sheep (1:400, Abcam).

For colocalization and morphological analysis, images of the CA1 area were acquired using a confocal laser scanning microscope (Zeiss, LSM 800). To analyse morphological indicators of microglial cells, iba-1-positive cells were selected. The soma area and ramification area were measured as previously described.[21] To count the branches of the microglial, images were analysed by the following steps with ImageJ: the threshold was set to visualize all processes, noise despeckling was performed, and the images were converted to binary images and then skeletonized using the appropriate plug-in in ImageJ.

Golgi staining and analysis

Golgi staining was performed by using the FD Rapid GolgiStain Kit (FD Neuro Technologies) according to the manufacturer's instructions to histologically examine dendritic spines by light microscopy. Briefly, mice brains were rapidly removed, and then transferred to an impregnation solution (A solution + B solution, premixed 24 h before) for two weeks in the dark. The brains were transferred to solution C and immersed for at least 72 h in the dark at RT. Then, the brains were cut into 150-μm sections using a vibrating microtome (Leica, VT 1000S). The sections were then mounted on gelatin-coated slides (FD Neuro Technologies) with solution C and dried at RT overnight. The staining procedure was as follows: the sections were immersed in a mixture of solution D, solution E and dd water (1:1:2) for 10 min, dehydrated in graded solutions of ethanol, and cleared in xylene solution before being mounted with neutral balsam.

The dendritic complexity of pyramidal neurons and the density of the spines on secondary dendrites were analysed using ImageJ. Branching was calculated by Sholl analysis. Concentric circles 10 μm apart and centred around the soma were drawn, and the number of intersections with the circles was quantified. Images of the spines were produced by merging several microscopic photos taken with a 100 × oil immersion lens, the number of spines was counted in ImageJ, and the number of spines/10 μm length was calculated.

Electron microscopy

Mice were perfused fixed with 2.5% glutaraldehyde under anaesthesia, and the hippocampi were fully separated from the brains, dissected into 1 mm³ pieces, and then immersed in 4% glutaraldehyde at 4 °C. The samples were post-fixed in 1% osmium tetroxide solution for 2 h. The samples were extensively washed three times with dd water and then dehydrated with increasing concentrations of ethanol (50%, 70% and 90%) and acetone (90% and 100%). Then, the samples were incubated and embedded in propylene oxide.

Ultrathin sections with a thickness of 60 nm were generated and then contrasted with uranyl acetate and lead citrate before imaging. Images were obtained using a transmission electron microscope (H-7500) at 100 KV and photographed using a Gatan-780 CCD camera. Images were taken at magnifications of 15,000x and 30,000x for analysis.

Glucose tolerance test

An intraperitoneal glucose tolerance test (ipGTT) was performed at two time points: after 12 weeks of HFD feeding (before AAV-TREM2 delivery) and after 45 weeks of HFD feeding (after TREM2 delivery). The mice were injected with glucose (2 g/kg, 25% w/v. D-glucose, Sigma) in 0.9% w/v NaCl after overnight fast. Blood glucose levels (mM) were measured with a glucometer (Roche) before (0 min) and 15, 30, 60 and 120 min after injection.

Statistical analysis

All data are presented as the means $\pm$ SEM. Statistical comparisons were performed using SPSS 19.0 (SPSS Inc.). The data were first tested for equal variance and normality, and the appropriate statistical tests were chosen. Comparisons of two groups were analysed by two sample t-test. Comparisons among multiple groups were calculated by one-way ANOVA followed by Tukey post hoc analysis and Dunnett T3 analysis. Repeated-measures ANOVA with Bonferroni post hoc test was used to analyse latencies in the MWM. The level of significance was set at 0.05.

Results

Hippocampal TREM2 overexpression does not alter the body weight and glucose tolerance in HFD-fed mice

HFD feeding induced persistent weight gain (Fig. S1A) and impaired glucose tolerance, inducing a greater increase in blood glucose levels after the intraperitoneal injection of glucose and a slower rate of glucose clearance (Fig. S1B) after 12 weeks of HFD feeding. To examine whether hippocampal TREM2 is related to cognitive impairments in T2DM, AAV-TREM2 and AAV-con were delivered to the bilateral hippocampus of HFD-fed mice (HFD-TREM2 or HFD-con) and NCD-fed mice (NCD-con) 36 weeks after dietary intervention. The baseline body weights and cognitive behavioural performance of HFD-TREM2 and HFD-con mice were comparable (Fig. S2). The mRNA and protein levels of TREM2 in the hippocampus of HFD-TREM2 mice were significantly elevated, as detected by RT-qPCR and Western blotting, respectively (Fig. S1C, Fig. 2A). The successful overexpression of TREM2 in microglia was confirmed by using double-labelling immunofluorescence with iba-1 (a calcium-binding protein specific for microglia, Fig. 2B). The final body weights did not differ between HFD-TREM2 mice and HFD-con mice (Fig. 2C). In addition, according to the ipGTT and the corresponding area under the curve (AUC), TREM2 treatment did not change glucose homeostasis

(Fig. 2D). These data suggest that hippocampal TREM2 overexpression did not alter the peripheral metabolic index.

Hippocampal TREM2 overexpression ameliorates cognitive impairment induced by long-term HFD feeding

To test whether long-term HFD feeding alters cognitive behaviour, the MWM, Y maze and NOR test were performed to assess spatial learning and memory, short-term spatial memory and recognition memory, respectively, after 28 weeks of HFD feeding (Fig. S3). Mice fed a HFD exhibited an increased latency to reach the hidden platform in the acquisition phase of the MWM (day 1 to day 5) (Fig. S3A, B and E), a lower number of platform crosses and decreased path length in the target (northwest, NW) quadrant in the probe test of the MWM (Fig. S3C–E). In addition, HFD mice showed a reduced spontaneous alternation rate and preference index in the Y maze and NOR test (Fig. S3F, G). 10 weeks after the intracerebral injection of AAV-TREM2 or AAV-con, the same behavioural tests were performed to examine alterations in cognitive function. HFD-TREM2 mice showed significant amelioration of hippocampal cognitive function compared with that of HFD-con mice, a shorter latency in the acquisition phase, and a greater number of platform crosses and longer path length in the target (southwest, SW) quadrant in the MWM (Fig. 3A–E), an increased alternation rate in the Y maze (Fig. 3F), an increased preference index in the NOR test (Fig. 3G). Thus, the results of the cognitive behavioural tests demonstrate that TREM2 overexpression in the hippocampus markedly attenuates the cognitive impairment induced by long-term HFD feeding.

Hippocampal TREM2 overexpression normalizes dendritic complexity and spine density in HFD-fed mice

Long-term HFD feeding causes a reduction in dendrites and spines, which are the foundational structures of memory and learning.[11] Golgi staining is widely used to evaluate dendritic complexity and spine density. Coronal sections of the hippocampus were made to determine the dendritic complexity of pyramidal cells in the CA1 region (Fig. 4A), dendritic branches were skeletonized and dendritic arborizations were quantified using ImageJ (Fig. 4B). Pyramidal cells from HFD-TREM2 mice exhibited a more complex branching pattern than those from HFD-con mice in regions 40 μm, 60 μm, 70 μm and 80 μm from the centre of soma (Fig. 4D). Similarly, there were more spines on the secondary dendrites of pyramidal cells from HFD-TREM2 mice than on those from HFD-con mice, as quantified by the number of spines per 10 μm (Fig. 4C, E). These results of Golgi Staining indicate that TREM2 overexpression in the hippocampus partly restores dendritic morphology and spine density, which are damaged by long-term HFD feeding.
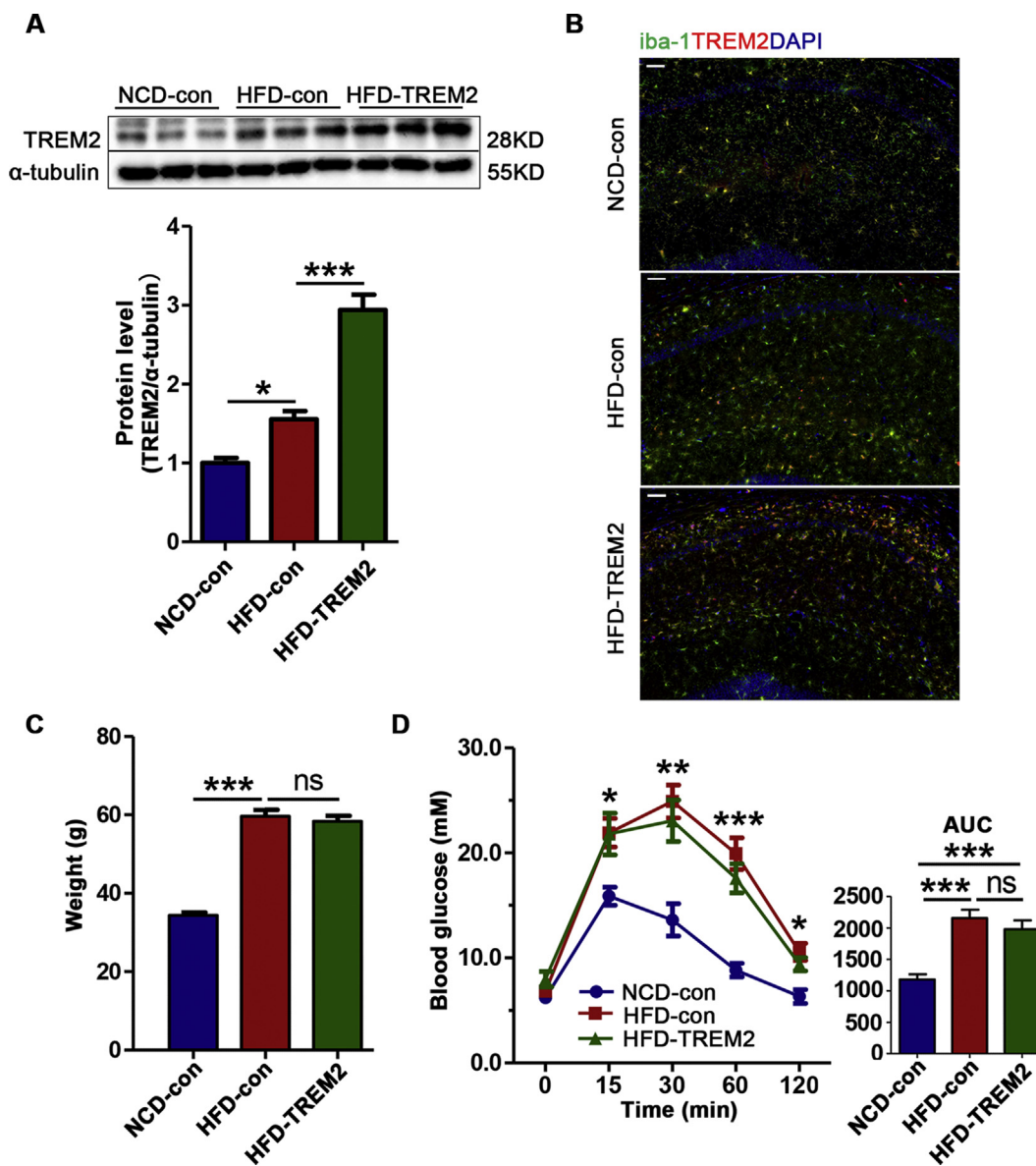
A

B

C

D

Figure 2 Hippocampal TREM2 overexpression does not alter the peripheral metabolic index. **(A)** TREM2 protein levels in the hippocampus 12 weeks after AAV delivery; $n = 6$ per group. **(B)** Double-labelling immunofluorescence for iba-1 (green) and TREM2 (red), with DAPI nuclear counterstain in the hippocampus after AAV delivery. Scale bar $= 50 \, \mu m$ **(C)** Body weights of the three groups 12 weeks after AAV-TREM2 or AAV-con injection; $n = 14$ per group. **(D)** Blood glucose levels and the corresponding area under the curve (AUC); there was no difference between HFD-TREM2 and HFD-con mice; $n = 6$ per group. The data represent the mean $\pm$ SEM, $*P < 0.05$, $**P < 0.01$, $***P < 0.001$, ns, no significance (one-way ANOVA with Tukey's post hoc test).

Hippocampal TREM2 overexpression ameliorates synaptic protein expression and synaptic ultrastructure

The difference in dendritic morphology and spine density between HFD-con and HFD-TREM2 mice indicates that the reinstatement of synaptic function was accompanied by a reversal of synaptic loss. Next, we quantified the synaptic protein levels in the hippocampus and observed the ultrastructure of synapses. Western blotting for synaptic proteins revealed that the expression of the presynaptic protein synaptophysin, the postsynaptic protein PSD95 and the scaffold protein spinophilin, which was markedly reduced in

HFD-con mice, was significantly upregulated in the hippocampal homogenates of HFD-TREM2 mice (Fig. 4F, G). To further observe the ultrastructure of the synapses in the hippocampus, we conducted electron microscopy. After long-term HFD feeding, the density of the synaptic connections and the number of synapses were decreased. These alterations were reversed by TREM2 overexpression, and the mice exhibited healthier synaptic ultrastructure, including more synapses and greater synaptic connection density (Fig. 4H). These results demonstrate that TREM2 overexpression in the hippocampus ameliorates synaptic protein levels and the ultrastructure of synapses, which are particularly important for cognitive function.
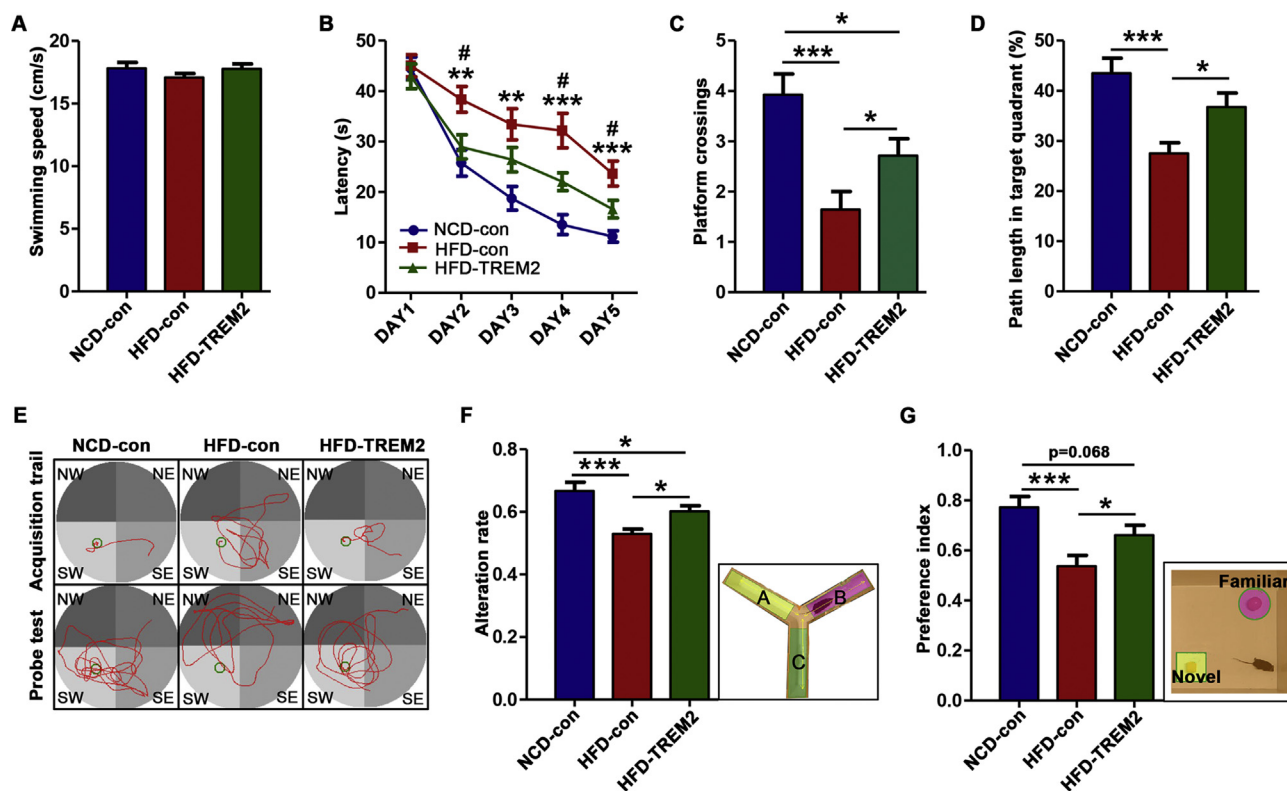
Figure 3 Hippocampal TREM2 overexpression ameliorates cognitive impairment induced by HFD feeding. **(A)** Swimming speed in the MWM. **(B)** The latency to reach the hidden platform in the acquisition period of the MWM after AAV injection. **(C)** The platform crossing number over 60 s during the memory trial in the MWM probe test. **(D)** The path length in the target (SW) quadrant in the probe test. NW, northwest; NE, northeast; SW, southwest; SE, southeast. **(E)** Representative samples of the path travelled during the acquisition period and probe test. The platform was located in the SW quadrant (green circle). **(F)** The rate of alternation was calculated as actual alternations/maximum alternations × 100%. **(G)** NOR preference index was determined by the formula TN/(TN + TF) with TN being the time spent exploring the novel object and TF being the time spent exploring the familiar object. $n = 14$ per group, the data represent the mean ± SEM, $*P < 0.05$, $**P < 0.01$, $***P < 0.001$ (one-way ANOVA with Tukey's post hoc test (A, C, D, F, G); repeated-measures ANOVA with Bonferroni post hoc test (B)).

TREM2 regulates microglial polarization and inhibits microglial activation

Different microglial phenotypes perform opposing functions, in brief, M1 microglia have a proinflammatory effect, and M2 microglia have an anti-inflammatory effect. Inducible nitric oxide synthase (iNOS) and arginase-1 (Arg-1) were used as the marker of M1 and M2 phenotype microglia, respectively. Surprisingly, a large number of microglia cells in the hippocampus, into which AAV-TREM2 was injected, were both iba-1- and Arg-1-positive (Fig. 5A, B). Next, we tried to determine whether this intervention affected the expression of the M1 marker iNOS. As expected, long-term HFD feeding increased the number of both iba-1- and iNOS-positive microglia in the hippocampus, but this number was decreased after TREM2 overexpression (Fig. 6A, B). By using RT-qPCR, we determined that the mRNA levels of the M2 markers *Arg-1* and *YM1/2* were also increased and that the levels of the M1 marker *Il-1β* was decreased in the hippocampus of HFD-TREM2 mice, even though there is no statistical difference in *iNOS* ($P = 0.067$) and *TNF-α* ($P = 0.055$) (Fig. 7C). In total, the double-staining immunofluorescence and RT-qPCR experiments demonstrate that the overexpression of TREM2 promotes the polarization of microglia to the M2 phenotype.

Microglial activation under inflammation is classically characterized by the increased number, also the retraction of processes and the growth of cell body size for highly plastic feature.[11,22] We examined the number and morphology of iba-1-positive microglia in the CA1 region of the hippocampus. There were fewer iba-1-positive microglia in hippocampal sections from HFD-TREM2 mice than in hippocampal sections from HFD-con mice (Fig. 6C), and morphology analysis of microglia demonstrated a lower morphological index with significantly increased arborization area in HFD-TREM2 mice (Fig. 6D–F). Therefore, these results indicate that TREM2 overexpression in the hippocampus inhibits microglial activation.

TREM2 overexpression suppresses the NF-κB pathway and neuroinflammation in the hippocampus of HFD mice

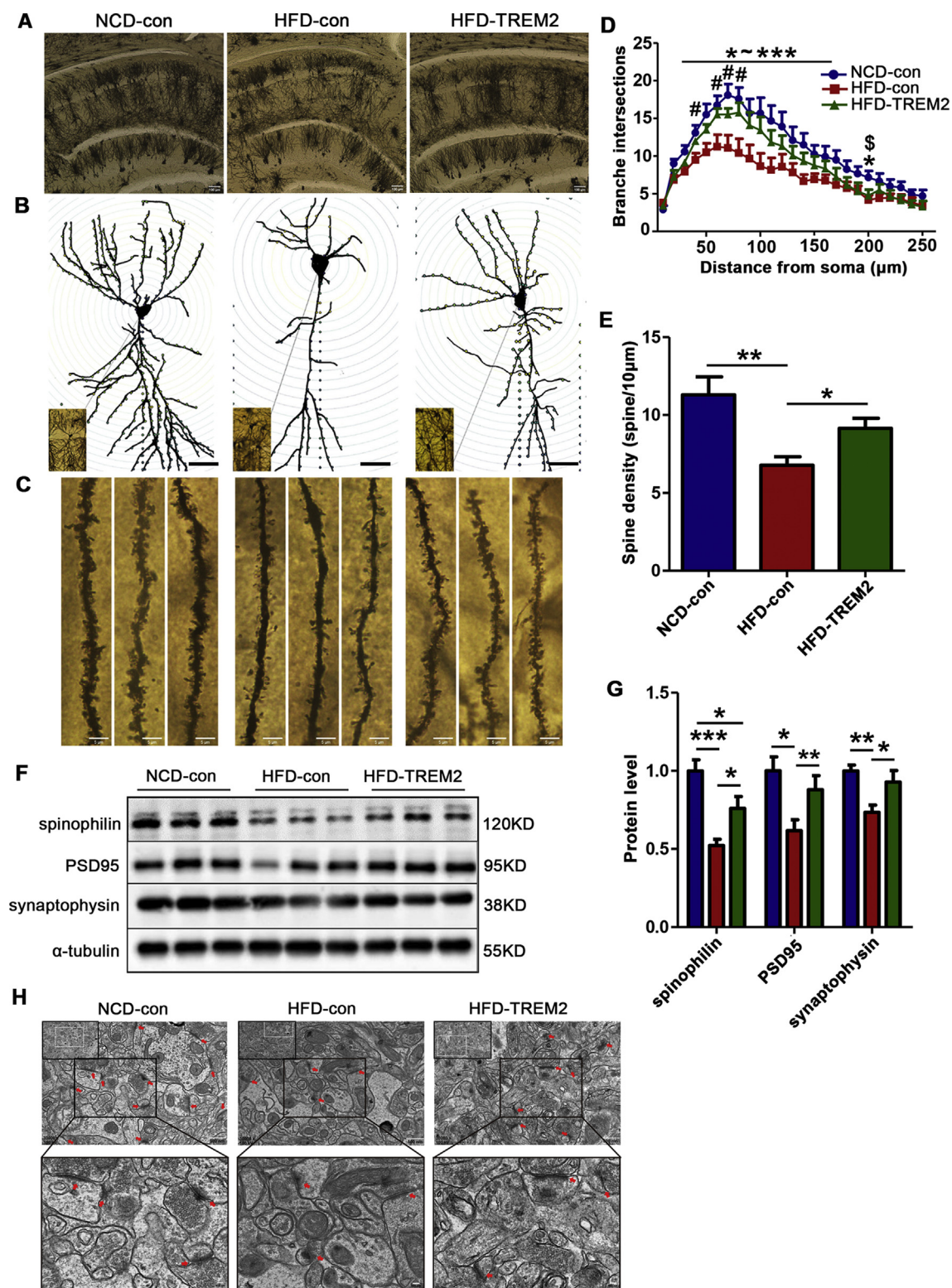As an innate immune receptor, TREM2 has been reported to be a negative regulator of the NF-κB inflammatory

Figure 4 Hippocampal TREM2 overexpression rescues dendritic morphology, synaptic protein expression and synapse ultrastructure. **(A)** Representative microphotographs of the Golgi-stained hippocampus of NCD-con, HFD-con and HFD-TREM2 mice. Scale bar = 100 μm. **(B, D)** Representative skeletonized CA1 pyramidal neurons in the hippocampus and Sholl analysis of the dendritic complexity of CA1 pyramidal neurons; $n = 3$ mice, 12 neurons per group. Scale bar = 20 μm *$P < 0.05$, ***$P < 0.001$ NCD-con vs HFD-con, #$P < 0.05$ HFD-TREM2 vs HFD-con, $$P < 0.05$ NCD-con vs HFD-TREM2. **(C, E)** Representative microphotographs of the spines on secondary dendrites of CA1 pyramidal neurons in the hippocampus. The quantification of spine density revealed a significant increase in HFD-TREM2 mice compared with HFD-con mice; $n = 3$ mice, 12 dendrites per group, Scale bar = 5 μm. **(F, G)** Western blot membranes depicting representative band intensities for the postsynaptic marker PSD95, the presynaptic marker
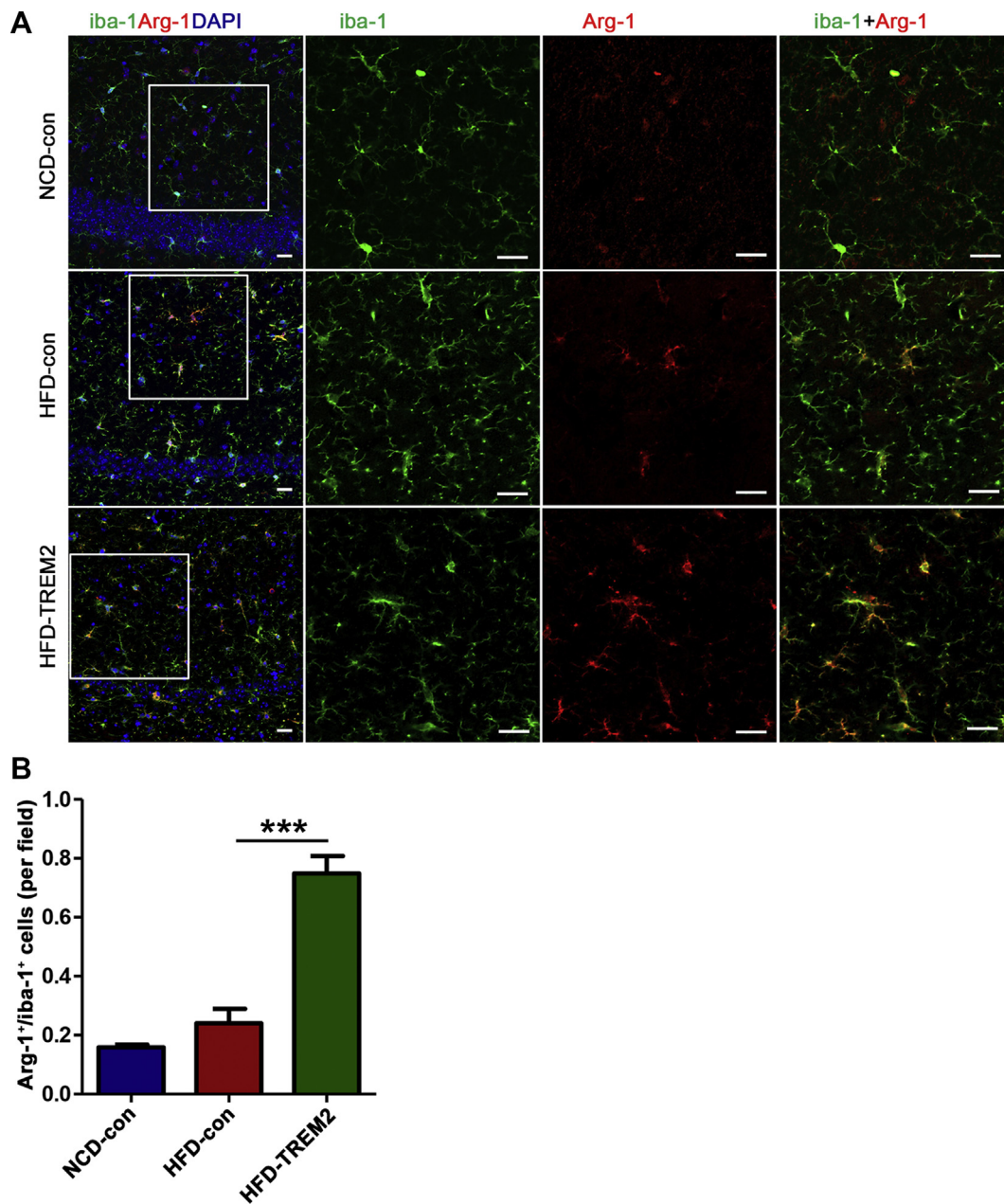
Figure 5 TREM2 overexpression increases the number of Arg-1-positive microglia in the hippocampus. **(A)** Double-staining immunofluorescence for iba-1 (green) and Arg-1 (red) with DAPI nuclear counterstain in the CA1 area of hippocampus. The left panel show 200× confocal images from the three groups. The right three panels show 400x confocal images of the partially enlarged details of the white pane. Scale bar = 20 μm. **(B)** The number of Arg-1-positive cells/the number of iba-1-positive cells per field; $n = 3$ mice, 6–9 fields per group. The data represent the mean ± SEM, ***$P < 0.001$ (one-way ANOVA with Dunnett T3 post hoc test).

signalling pathway in other experimental models.[23,24] To determine whether the overexpression of TREM2 affects NF-κB signalling in our model, we examined the activation of the NF-κB signalling pathway. Our results revealed that, in the long-term HFD feeding model, the phosphorylation of p65 and IkB-α was significantly enhanced in the hippocampus, while TREM2 overexpression attenuated the phosphorylation of p65 and IkB-α (Fig. 7A, B), which correlated with the decreased mRNA levels of *TLR-4* and *IL-1β* (Fig. 7C).

---

synaptophysin and the scaffolding protein spinophilin; $n = 6$ per group. **(H)** Representative ultrastructure image showing more synapses and healthy synapse structure in HFD-TREM2 mice relative to HFD-con mice. Scale bar = 500 nm. The data represent the mean ± SEM, *$P < 0.05$, **$P < 0.01$, ***$P < 0.001$ (one-way ANOVA with Tukey's post hoc test (D, G); one-way ANOVA with Dunnett T3 post hoc test (E)).
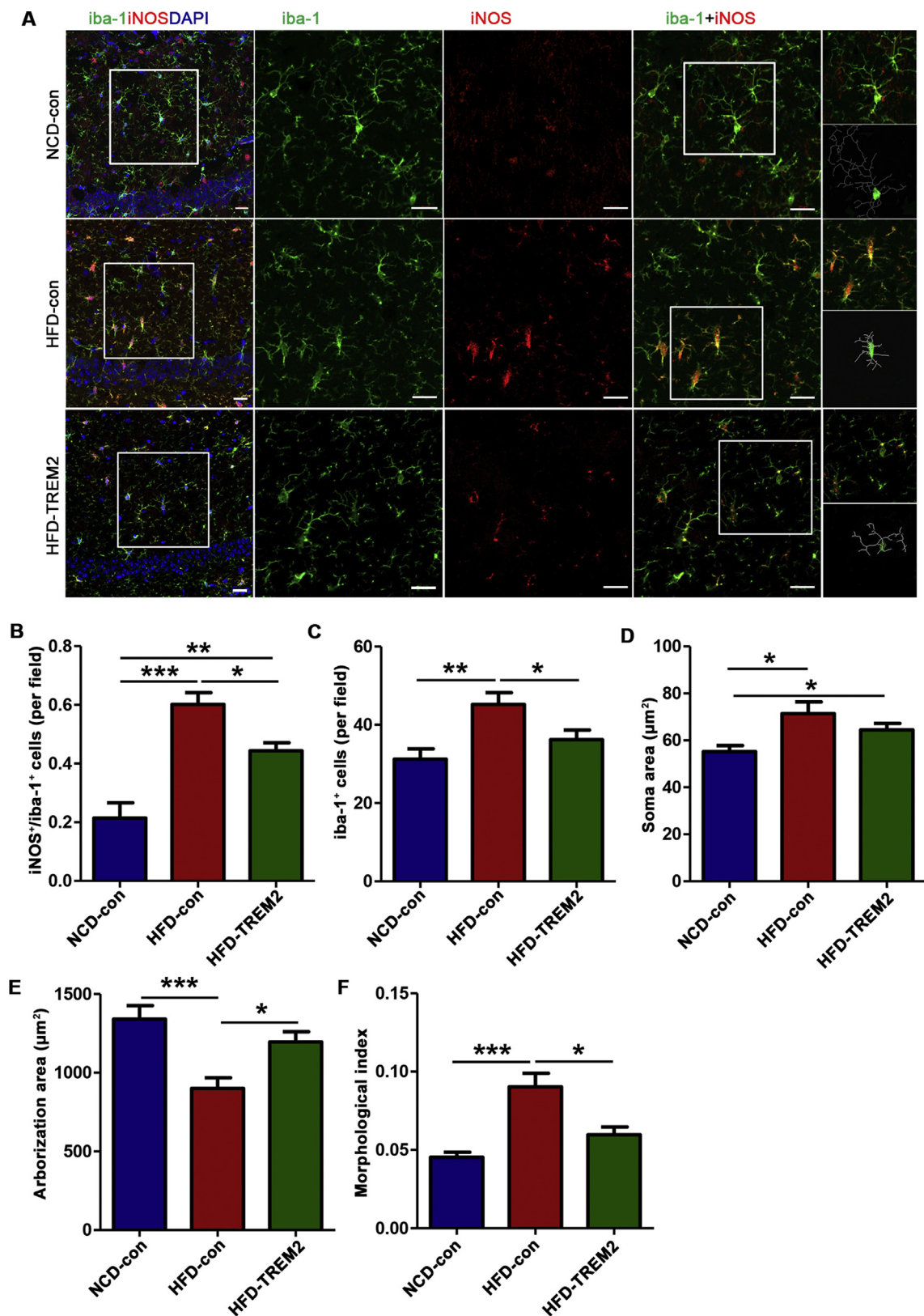
Figure 6 TREM2 overexpression decreases the number of iNOS-positive microglia and inhibits microglial activation. **(A)** Representative images of double-staining immunofluorescence for iba-1 (green) and iNOS (red) with DAPI nuclear counterstain in the CA1 area of the hippocampus. The left panels show 200x confocal images from the three groups. The middle three panels show 400x confocal images of iba-1, iNOS and iba-1+iNOS immunofluorescence. The right panels show representative double-stained single microglial cell and the corresponding skeleton reconstruction of the microglia. Scale bar = 20 μm. **(B)** The number of iNOS-positive

Discussion

The present study demonstrates that hippocampal TREM2 overexpression protected mice against cognitive impairment induced by long-term HFD feeding. Mice on a long-term HFD showed impaired dendritic complexity, diminished synaptic proteins, abnormal synaptic ultrastructure and upregulated neuroinflammation in the hippocampus in addition to well-characterized metabolic abnormalities. However, hippocampal microglial TREM2 overexpression obviously ameliorated these detrimental changes and rescued cognitive decline, without significant effects on body weight or glucose homeostasis in the periphery. The neuroprotective effect of TREM2 in long-term HFD mice is related to its inhibition of neuroinflammation, regulation of microglial phenotype and activation.

Rare variants of TREM2, which increase the risk of developing AD, are thought of as loss of function variants.[25] In this study, we found that both the mRNA and protein levels of TREM2 were upregulated in the hippocampus of mice fed a long-term HFD. This is consistent with previous immunofluorescence results in the hippocampus of mice fed a chronic western diet (WD) for 8 months.[26] However, other report showed that the mRNA level of TREM2 in the hypothalamus was not changed after acute HFD exposure for 3 days but that was downregulated when the HFD exposure was 8 weeks.[27] These different results might be attributed to the different ages of the mice used and the different brain regions evaluated in the two studies. During the process of physiological aging, the expression of microglial TREM2 also changed, although the results are controversial. The microglial TREM2 mRNA increased by 50–100% from 50 to 90 years of age without obvious pathological processes in human, but decreased in 24-month-old mice.[3,28] However, the present study cannot explain why TREM2 levels are elevated after long-term HFD, since we also found that the mRNA level of TREM2 was decreased when BV-2 cells were stimulated with LPS or high concentrations of insulin (data not shown). Researches consider that the TREM2 expression is decreased by proinflammatory stimuli *in vitro* but is almost universally increased *in vivo* in inflammatory context and different disease states.[29] Moreover, the protective effect of TREM2 in both AD model and our model might reflect a hypothesis of compensatory response for homeostatic alterations in the CNS. This hypothesis is supported by a cross-sectional multicentre study, which illustrated that the levels of sTREM2, a soluble form of TREM2 derived from proteolytic cleavage of TREM2, changes in the cerebrospinal fluid (CSF) in AD in a disease progression-dependent manner, reaching the highest level in the mild cognitive impairment (MCI) stage and then decreasing in the dementia stage.[30,31] Similarly, sTREM2 levels in the CSF have also been found to be elevated in non-obese diabetes patients with

cognitive impairment.[32] For current understanding, TREM2 signalling is essential for microglia to maintain CNS homeostasis.[33] The increased TREM2 expression may reflect the compensatory response to the damage of brain homeostasis in our HFD intervention model, and the further overexpression of TREM2 may work in coordination with the original effect of TREM2 to maintain homeostasis. The same effect of TREM2 is observed in APP/PS1dE9 AD model. In the brain of APP/PS1dE9 mice, TREM2 level is elevated by Aβ stimulation, then further TREM2 overexpression showed neuroprotective effect and ameliorated cognitive impairment.[34] However, many questions still exist, and further study is warranted to understand the potential mechanism of upregulation of TREM2 under HFD in order to better understand the role of TREM2 in cognitive regulation.

Our findings are in agreement with the observation that diet-induced obesity mice exhibit fewer dendritic spines in pyramidal cells in the CA1 region and decreased synaptic proteins expression in hippocampus.[11,35] As the macrophages of the brain, microglia are known to substantial activation in response to the pathological states result in a transformation into an ameboid morphology and ultimately result in neurotoxicity or neuroprotection.[36,37] Morphological changes of microglia are related to synapse loss in the medial prefrontal cortex in obesity rats with cognitive decline.[38] Another study shown that the microglia isolated from obese mice are capable of internalizing synaptosomes and the microglial cells lost its anatomical complexity.[11] The uncontrolled activated microglia are shift to a pathological state and engulf other functional synapses after long-term HFD feeding. When the activation of microglia is blocked by using minocycline (the antibiotic been used to pharmacologically inhibit microglial activation) or the partial knockdown of Cx3cr (fractalkine receptor), dendritic spine loss and cognitive decline are reversed in obese mice.[35] In our long-term HFD consumption model, TREM2 overexpression inhibits the activation of microglia and maintains the ramified feature of microglia, and partially reverses the damage of dendrites and synapses. Since there is no clear evidence for the interaction between TREM2 and iba-1, these results may indicate that TREM2 promotes microglia fitness, maintains CNS homeostasis and ultimately inhibit the overactivation of microglia in HFD-fed mice. Moreover, microglia play a critical role in neuronal development and shaping neural circuits in healthy brain, and recent study imply that TREM2 is a critical molecule for appropriate synaptic refinement during neurodevelopment, and TREM2 deficiency affect the number of synapses across brain regions.[39]

Microglia act as a double-edged sword to exert neurotoxic and neuroprotective functions in the CNS depending on the polarization phenotype. iNOS and Arg-1 are recommended to be relatively straightforward markers of the M1 and M2 phenotypes, respectively.[40] Long-term HFD feeding

cells/the number of iba-1-positive cells per field; $n = 3$ mice, 9 fields per group (one-way ANOVA with Tukey's post hoc test). **(C)** The number of iba-1-positive cells per field; $n = 3$ mice, 9 fields per group (one-way ANOVA with Tukey's post hoc test). **(D-G)**. Quantitative analysis of microglial morphology, the soma area of the microglia (D), the arborization area of the microglia (E), and the morphological index (soma area/arborization area) (F) and Sholl analysis of the average number of branches per microglial cell (G); $n = 3$ mice, 12 fields, 30 cells per group (one-way ANOVA with Dunnett T3 post hoc test). The data represent the mean $\pm$ SEM, *$P < 0.05$, **$P < 0.01$, ***$P < 0.001$.
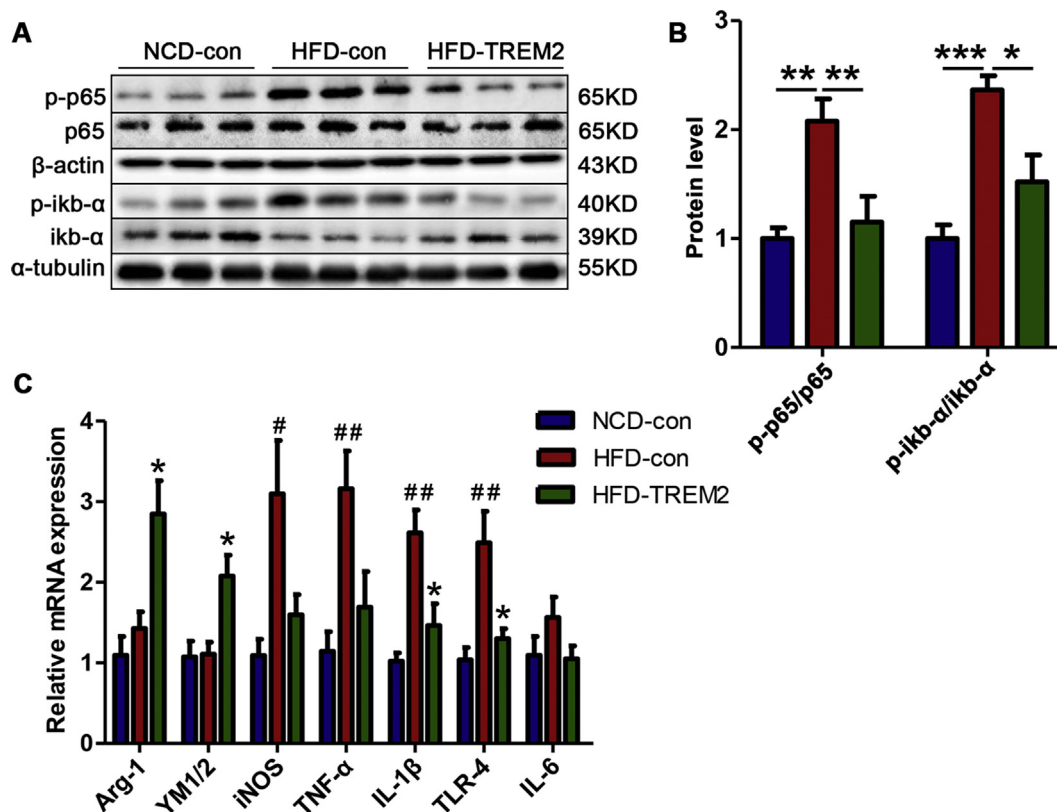
Figure 7 TREM2 overexpression suppresses NF-κB activation and neuroinflammation in the hippocampus. **(A, B)** Western blot membranes depicting representative band intensities for p65, p-p65, IkB-α, and p-IkB-α; normalize to β-actin and α-tubulin; $n = 6$ per group. **(C)** Relative mRNA levels of the M1 markers and proinflammatory factors *iNOS, TNF-α, IL-1β, TLR-4* and *IL-6* and the M2 markers *Arg-1* and *YM1/2*; $n = 5$ per group, asterisks (*) vs HFD-con, asterisks (#) vs NCD-con. The data represent the mean ± SEM, */#$P < 0.05$, **/##$P < 0.01$, ***$P < 0.001$ (one-way ANOVA with Tukey's post hoc test).

evidently increased the number of M1 phenotype microglia in the hippocampus; however, the overexpression of TREM2 skewed microglial polarization towards the M2 phenotype in our study. The lack of M2 microglial cells not only fails to control neuroinflammation but also results in lower levels of neuroprotective factors.[40] In other animal models, i.e. cerebral ischemia, spinal cord injury and multiple sclerosis, M2-polarized microglia exhibit anti-inflammatory effect and promote neurite outgrowth.[41–43] In AD model, the neuroprotective effects of M2 phenotype microglia are mainly related to the secretion of anti-inflammatory cytokines and the enhancement of phagocytic function.[44] The enhanced phagocytic function of microglia is beneficial to the clearance of amyloid-β (Aβ), while the role of M2 microglia in synaptic internalization has not been reported and requires further discussion. Recent study has also found that M2 microglia-derived exosomes promote neuronal survival and protect the brain from damage.[45]

Elevated pro-inflammation in the hippocampus was reported consequently lead to neuronal impairment.[46] Mice maintained on long-term HFD exhibited an apparent inflammatory response in the hippocampus, as the mRNA levels of *IL-1β, TNF-α, TLR-4* and *iNOS* were significantly higher in these mice than in NCD-fed mice. This change was accompanied by an increase in the number of iNOS-positive microglia. The overexpression of

TREM2 led to a reduction in the mRNA levels of *IL-1β* and *TLR-4*, the elevation in the number of Arg-1-positive microglia and mRNA levels of *Arg-1* and *YM1/2*. These results imply that TREM2 suppressed neuroinflammation by switching microglia towards the M2 phenotype. The activation of NF-κB is a characteristic marker of M1 polarization and is involved in obesity-associated neuroinflammation, and its signalling has been implicated in cytokine production, synaptic plasticity.[46] The overexpression of TREM2 alleviated the phosphorylation of p65 and IkB-α in the hippocampus, and thus related to the ameliorated neuroinflammation induced by HFD. However, the molecular mechanism of anti-inflammatory effect of TREM2 still needs further study.

In conclusion, our current study is the first to show that the hippocampal overexpression of TREM2 rescues cognitive impairment after long-term HFD consumption. The protective effect of TREM2 is likely attributable to the promotion of microglial M2 polarization and the suppression of the activation of microglia and neuroinflammation. The study highlights the role of innate immunity in obesity/diabetes-associated cognitive impairment, suggests that TREM2 might be a novel target for the intervention of obesity/diabetes-associated cognitive impairment and establishes a connection between obesity/diabetes-related neurodegeneration and AD.

Conflict of interests

Funding

Appendix A. Supplementary data

Supplementary data to this article can be found online at https://doi.org/10.1016/j.gendis.2020.05.005.

References

1. Guerreiro R, Wojtas A, Bras J, et al. TREM2 variants in Alzheimer's disease. *N Engl J Med*. 2013;368(2):117–127.
2. Jonsson T, Stefansson H, Steinberg S, et al. Variant of TREM2 associated with the risk of Alzheimer's disease. *N Engl J Med*. 2013;368(2):107–116.
3. Hickman SE, Kingery ND, Ohsumi TK, et al. The microglial sensome revealed by direct RNA sequencing. *Nat Neurosci*. 2013;16(12):1896–1905.
4. Nizami S, Hall-Roberts H, Warrier S, Cowley SA, Di Daniel E. Microglial inflammation and phagocytosis in Alzheimer's disease: potential therapeutic targets. *Br J Pharmacol*. 2019;176(18):3515–3532.
5. Wang Y, Cella M, Mallinson K, et al. TREM2 lipid sensing sustains the microglial response in an Alzheimer's disease model. *Cell*. 2015;160(6):1061–1071.
6. Ulland TK, Song WM, Huang SC, et al. TREM2 maintains microglial metabolic fitness in Alzheimer's disease. *Cell*. 2017; 170(4):649–663.
7. Keren-Shaul H, Spinrad A, Weiner A, et al. A unique microglia type Associated with restricting development of Alzheimer's disease. *Cell*. 2017;169(7):1276–1290.
8. Yang Y, Song W. Molecular links between Alzheimer's disease and diabetes mellitus. *Neuroscience*. 2013;250:140–150.
9. Guillemot-Legris O, Muccioli GG. Obesity-induced neuroinflammation: beyond the hypothalamus. *Trends Neurosci*. 2017;40(4):237–253.
10. Miller AA, Spencer SJ. Obesity and neuroinflammation: a pathway to cognitive impairment. *Brain Behav Immun*. 2014; 42:10–21.
11. Hao S, Dey A, Yu X, Stranahan AM. Dietary obesity reversibly induces synaptic stripping by microglia and impairs hippocampal plasticity. *Brain Behav Immun*. 2016;51:230–239.
12. Jha MK, Lee WH, Suk K. Functional polarization of neuroglia: implications in neuroinflammation and neurological disorders. *Biochem Pharmacol*. 2016;103:1–16.
13. Ajmone-Cat MA, Mancini M, De Simone R, Cilli P, Minghetti L. Microglial polarization and plasticity: evidence from organotypic hippocampal slice cultures. *Glia*. 2013;61(10): 1698–1711.
14. Zhang Y, Feng S, Nie K, et al. TREM2 modulates microglia phenotypes in the neuroinflammation of Parkinson's disease. *Biochem Biophys Res Commun*. 2018;499(4):797–802.
15. Jiang T, Zhang YD, Chen Q, et al. TREM2 modifies microglial phenotype and provides neuroprotection in P301S tau transgenic mice. *Neuropharmacology*. 2016;105:196–206.
16. Zhai Q, Li F, Chen X, et al. Triggering receptor expressed on myeloid cells 2, a novel regulator of immunocyte phenotypes, confers neuroprotection by relieving neuroinflammation. *Anesthesiology*. 2017;127(1):98–110.
17. Srinivasan R, Lu TY, Chai H, et al. New transgenic mouse lines for selectively targeting astrocytes and studying calcium signals in astrocyte processes in situ and in vivo. *Neuron*. 2016; 92(6):1181–1195.
18. Ji M, Xie XX, Liu DQ, et al. Hepatitis B core VLP-based misdisordered tau vaccine elicits strong immune response and alleviates cognitive deficits and neuropathology progression in Tau.P301S mouse model of Alzheimer's disease and frontotemporal dementia. *Alzheimer's Res Ther*. 2018;10(1):55.
19. Leger M, Quiedeville A, Bouet V, et al. Object recognition test in mice. *Nat Protoc*. 2013;8(12):2531–2537.
20. Vorhees CV, Williams MT. Morris water maze: procedures for assessing spatial and related forms of learning and memory. *Nat Protoc*. 2006;1(2):848–858.
21. Basilico B, Pagani F, Grimaldi A, et al. Microglia shape presynaptic properties at developing glutamatergic synapses. *Glia*. 2019;67(1):53–67.
22. Kettenmann H, Hanisch UK, Noda M, Verkhratsky A. Physiology of microglia. *Physiol Rev*. 2011;91(2):461–553.
23. Ren M, Guo Y, Wei X, et al. TREM2 overexpression attenuates neuroinflammation and protects dopaminergic neurons in experimental models of Parkinson's disease. *Exp Neurol*. 2018; 302:205–213.
24. Ito H, Hamerman JA. TREM-2, triggering receptor expressed on myeloid cell-2, negatively regulates TLR responses in dendritic cells. *Eur J Immunol*. 2012;42(1):176–185.
25. Cheng-Hathaway PJ, Reed-Geaghan EG, Jay TR, et al. The Trem2 R47H variant confers loss-of-function-like phenotypes in Alzheimer's disease. *Mol Neurodegener*. 2018;13(1):29.
26. Graham LC, Harder JM, Soto I, de Vries WN, John SW, Howell GR. Chronic consumption of a western diet induces robust glial activation in aging mice and in a mouse model of Alzheimer's disease. *Sci Rep*. 2016;6:21568.
27. Baufeld C, Osterloh A, Prokop S, Miller KR, Heppner FL. High-fat diet-induced brain region-specific phenotypic spectrum of CNS resident microglia. *Acta Neuropathol*. 2016;132(3): 361–375.
28. Forabosco P, Ramasamy A, Trabzuni D, et al. Insights into TREM2 biology by network analysis of human brain gene expression data. *Neurobiol Aging*. 2013;34(12):2699–2714.
29. Jay TR, von Saucken VE, Landreth GE. TREM2 in neurodegenerative diseases. *Mol Neurodegener*. 2017;12(1):56.
30. Suarez-Calvet M, Kleinberger G, Araque Caballero MA, et al. sTREM2 cerebrospinal fluid levels are a potential biomarker for microglia activity in early-stage Alzheimer's disease and associate with neuronal injury markers. *EMBO Mol Med*. 2016;8(5):466–476.
31. Suarez-Calvet M, Araque Caballero MA, Kleinberger G, et al. Early changes in CSF sTREM2 in dominantly inherited Alzheimer's disease occur after amyloid deposition and neuronal injury. *Sci Transl Med*. 2016;8(369):369ra178.
32. Tanaka M, Yamakage H, Masuda S, et al. Serum soluble TREM2 is a potential novel biomarker of cognitive impairment in Japanese non-obese patients with diabetes. *Diabetes Metab*. 2017;45(1):86–89.
33. Mecca C, Giambanco I, Donato R, Arcuri C. Microglia and aging: the role of the TREM2-DAP12 and CX3CL1-CX3CR1 Axes. *Int J Mol Sci*. 2018;19(1):318.
34. Jiang T, Tan L, Zhu XC, et al. Upregulation of TREM2 ameliorates neuropathology and rescues spatial cognitive impairment in a transgenic mouse model of Alzheimer's disease. *Neuropsychopharmacology*. 2014;39(13):2949–2962.

35. Cope EC, LaMarca EA, Monari PK, et al. Microglia play an active role in obesity-associated cognitive decline. *J Neurosci*. 2018; 38(41):8889–8904.

36. Neumann H, Kotter MR, Franklin RJ. Debris clearance by microglia: an essential link between degeneration and regeneration. *Brain*. 2009;132(Pt 2):288–295.

37. Wake H, Moorhouse AJ, Jinno S, Kohsaka S, Nabekura J. Resting microglia directly monitor the functional state of synapses in vivo and determine the fate of ischemic terminals. *J Neurosci*. 2009;29(13):3974–3980.

38. Bocarsly ME, Fasolino M, Kane GA, et al. Obesity diminishes synaptic markers, alters microglial morphology, and impairs cognitive function. *Proc Natl Acad Sci U S A*. 2015;112(51): 15731–15736.

39. Jay TR, Saucken VE, Muñoz B, et al. TREM2 is required for microglial instruction of astrocytic synaptic engulfment in neurodevelopment. *Glia*. 2019;67(10):1873–1892.

40. Cherry JD, Olschowka JA, O'Banion M. Neuroinflammation and M2 microglia: the good, the bad, and the inflamed. *J Neuroinflammation*. 2014;11(1):98.

41. Kigerl KA, Gensel JC, Ankeny DP, et al. Identification of two distinct macrophage subsets with divergent effects causing either neurotoxicity or regeneration in the injured mouse spinal cord. *J Neurosci*. 2009;29(43):13435–13444.

42. Hu X, Li P, Guo Y, et al. Microglia/macrophage polarization dynamics reveal novel mechanism of injury expansion after focal cerebral ischemia. *Stroke*. 2012;43(11):3063–3070.

43. Mikita J, Dubourdieu-Cassagno N, Deloire MS, et al. Altered M1/M2 activation patterns of monocytes in severe relapsing experimental rat model of multiple sclerosis. Amelioration of clinical status by M2 activated monocyte administration. *Mult Scler*. 2011;17(1):2–15.

44. Franco R, Fernandez-Suarez D. Alternatively activated microglia and macrophages in the central nervous system. *Prog Neurobiol*. 2015;131:65–86.

45. Song Y, Li Z, He T, et al. M2 microglia-derived exosomes protect the mouse brain from ischemia-reperfusion injury via exosomal miR-124. *Theranostics*. 2019;9(10): 2910–2923.

46. Lu J, Wu DM, Zheng YL, et al. Ursolic acid improves high fat diet-induced cognitive impairments by blocking endoplasmic reticulum stress and IkappaB kinase beta/nuclear factor-kappaB-mediated inflammatory pathways in mice. *Brain Behav Immun*. 2011;25(8):1658–1667.